IOPscience iopscience.iop.org

Home Search Collections Journals About Contact us My IOPscience

Characterization of deep wet etching of fused silica glass for single cell and optical sensor deposition

This article has been downloaded from IOPscience. Please scroll down to see the full text article.

2009 J. Micromech. Microeng. 19 065013

(http://iopscience.iop.org/0960-1317/19/6/065013)

The Table of Contents and more related content is available

Download details:
IP Address: 149.169.217.80
The article was downloaded on 30/03/2010 at 17:46

Please note that terms and conditions apply.

IOP PUBLISHING JOURNAL OF MICROMECHANICS AND MICROENGINEERING

J. Micromech. Microeng. **19** (2009) 065013 (8pp) doi:10.1088/0960-1317/19/6/065013

Characterization of deep wet etching of fused silica glass for single cell and optical sensor deposition

Haixin Zhu[1], **Mark Holl, Tathagata Ray, Shivani Bhushan and Deirdre R Meldrum**

Center for Ecogenomics, The Biodesign Institute, Arizona State University, Tempe, AZ 85287, USA

E-mail: Haixin.zhu@asu.edu

Received 17 December 2008, in final form 12 March 2009
Published 20 May 2009
Online at stacks.iop.org/JMM/19/065013

Abstract

The development of a high-throughput single-cell metabolic rate monitoring system relies on the use of transparent substrate material for a single cell-trapping platform. The high optical transparency, high chemical resistance, improved surface quality and compatibility with the silicon micromachining process of fused silica make it very attractive and desirable for this application. In this paper, we report the results from the development and characterization of a hydrofluoric acid (HF) based deep wet-etch process on fused silica. The pin holes and notching defects of various single-coated masking layers during the etching are characterized and the most suitable masking materials are identified for different etch depths. The dependence of the average etch rate and surface roughness on the etch depth, impurity concentration and HF composition are also examined. The resulting undercut from the deep HF etch using various masking materials is also investigated. The developed and characterized process techniques have been successfully implemented in the fabrication of micro-well arrays for single cell trapping and sensor deposition. Up to 60 μm deep micro-wells have been etched in a fused silica substrate with over 90% process yield and repeatability. To our knowledge, such etch depth has never been achieved in a fused silica substrate by using a non-diluted HF etchant and a single-coated masking layer at room temperature.

(Some figures in this article are in colour only in the electronic version)

1. Introduction

Developments in single-cell metabolic rate monitoring systems with fmol/minute resolution are essential to the real-time investigations of cellular heterogeneity using experiments that examine cell damage and death pathways including neoplastic progression as seen in cancer or pyroptosis and in heart disease and stroke [1]. As part of the single cell analysis system, the fluorescent sensing systems based on the transparent cell-trapping platform are becoming increasingly popular due to the inherent difficulties associated with other measurements at the required detection resolution [2–6]. Borosilicate glass has been used as the common substrate material for this cell-trapping platform because of its high optical transparency and the ability to withstand many environmental influences such as O_2 permeation [7]. To acquire high throughput device prototyping at the micro-meter scale, the silicon micromachining techniques (lithography/wet etch) commonly used in the semiconductor industry are selected to fabricate a micro-well array for a single cell and sensor deposition. However, the surface roughness resulting from the glass etch is relatively high due to the impurity local masking effect which may increase the micro-well volume variation from well to well. On the other hand, the high impurity concentration inside the borosilicate glass makes it incompatible with many standard CMOS (complementary metal-oxide-semiconductor) processes such as high temperature processes (annealing and chemical vapor

[1] Address for correspondence: Center for Ecogenomics, The Biodesign Institute at Arizona State University, Arizona State University, Tempe, AZ 85287-9709, USA.

 © 2009 IOP Publishing Ltd Printed in the UK

Table 1. Normalized chemical composition of selected glass substrates.

	SiO_2	B_2O_3	Na_2O	K_2O	Al_2O_3	ZnO	TiO_2	Others
D-263	64.1%	8.4%	6.4%	6.9%	4.2%	5.9%	4.0%	0.1%
Pyrex 7740	80.9%	12.7%	4%	0.04%	2.3%			
Fused silica	∼100%							

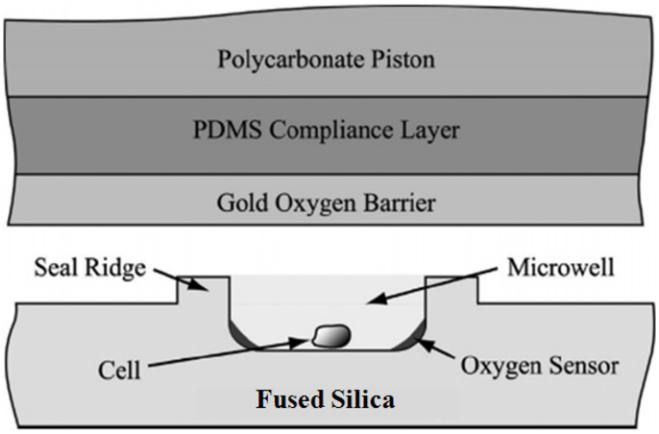

Figure 1. Illustrative side view of the micro-well, sensor and lid. The cells are trapped inside the micro-well with the sensors seating on the corner of the wells; the piston brings down the lid and closes the micro-well. The sensor excitation and imaging occur through the bottom of the glass chip [7].

deposition) and RIE (reactive ion etch) due to the low thermal stability and process contamination issues. This highly reduces the process flexibility and limits the device design complexity.

Among all types of alternative transparent substrates, fused silica is a very attractive material since besides all the desired properties borosilicate glass has, it also has excellent thermal stability and high purity (∼100% silicon dioxide). Therefore, it eliminates the contamination issues during the process and is fully CMOS process compatible. Since the application of fused silica for single cell trapping and sensor deposition requires the formation of 30–40 μm deep micro-wells with 60–100 μm well diameter for the purpose of reliable cell confinement and 3–5 μm tall surrounding lips for the purpose of complete gas sealing (figure 1), a suitable etch technology targeting >30 μm deep fused silica etch is needed.

Wet chemical etch and plasma dry etch are the most widely used techniques to structure the fused silica substrate. By using a thick metal mask and high density plasma reactive ion etcher, up to 50 μm deep trenches have been dry etched in fused silica [8]. However, this approach requires expensive equipments and high-selectivity masking material, and the resulting etch rate is low (<190 nm min^{-1}) which highly lowers the process throughput. On the other hand, wet etch methods using various diluted HF at elevated temperature are also studied [9–12]. In these approaches, the acquired etch rate increases to 340 nm min^{-1} at 47 °C, and the etch process takes hours to get the desired etch depth. Though this approach relaxes the requirement on the masking material compared to the dry etch approach, the resulting etch rate is still low, and HF etching at elevated temperature brings up the concerns of the processing safety.

In this paper, we report our results from the bulk etching of fused silica in an HF-based etchant at room temperature using a single-coated masking layer. The focus is on the characterization of single-layer masking material, etch rate, average surface roughness and undercut. Three major types of masking material, including photoresist (PR), metal and silicon-based thin film, are studied, and the best masking material is proposed. The effect of the micro-well size, etchant concentration on the etch rate and surface roughness are also included in this study. For comparison, the results from impure glass substrates (D-263 and Pyrex 7740) are also included. The acquired results and developed techniques are successfully applied in the fabrication of a micro-well array for single cell trapping and sensor deposition and can also be easily applied in any other glass-based chip fabrication using wet-etch techniques.

All processes presented in this paper are performed using the class 100 cleanroom facilities provided by the Center for Solid State Electronics Research (CSSER) in Arizona State University.

2. Methods and process techniques

2.1. Materials

4 inch double-side polished fused silica wafers (Markoptics, Santa Ana, CA) were selected as the processing substrate materials. To study the effect of impurity on the etch rate and roughness, 4 inch D-263 (Thermo Fisher Scientific, Portsmouth, NH) and Pyrex 7740 (Bullen Ultrasonics, Eaton, OH) substrates were also included. The chemical composition of the selected substrates is listed in table 1. Photoresists (AZP4620, AZ3312 and AZ 5214 from Mays Chemicals, Indianapolis, IN) were used as either the masking layer for glass etch or the sacrificial layer for photolithography. Various thin film layers (Au/Cr, Al, poly-si, silicon nitride and a-Si) were deposited onto the glass substrates as the hard masking material. A mixture of 16 parts of 85 wt% phosphoric acid and 1 part of 30 wt% nitric acid was used to wet etch the coated aluminum layer. A mixture of 3 parts of 35 wt% hydrochloric acid and 1 part of 60 wt% nitric acid was used to etch Au. A commercially available chrome etchant was used to etch the chrome layer. The hydrofluoric acid (49 wt%) both concentrated and diluted with DI water, or 35 wt% hydrochloric acid or 85 wt% phosphoric acid were used to etch micro-wells into glass substrates.

Table 2. Major process parameters for masking layer deposition.

Masking material	Deposition technique	Equipment	Major processing parameters
Photoresist	Spin-coat	SCS 7608D	
Aluminum	E-beam evaporation	CHA600-SE	5.4×10^{-6} Torr, 223 mA
Chromium			4×10^{-6} Torr, 11 mA
Gold			2×10^{-5} Torr, 119 mA
Silicon nitride	Low pressure chemical vapor deposition	Tystar MiniTytan	250 mT, 835 °C, 100 sccm SiH_2Cl_2, 20 sccm NH_3
Poly-silicon			300 mT, 650 °C, 60 sccm SiH_4
Amorphous silicon			300 mT, 560 °C, 60 sccm SiH_4

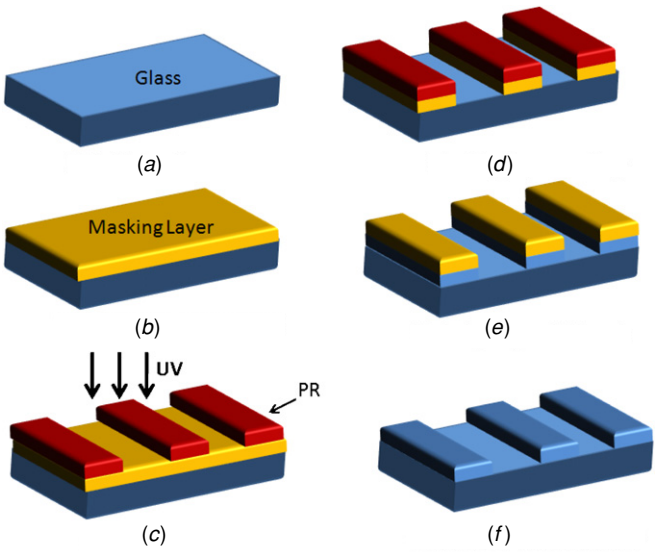

Figure 2. Typical process flow for micro-well fabrication (not scaled). (*a*) RCA wafer clean, (*b*) masking layer deposition, (*c*) photo-lithography, (*d*) masking layer etching, (*e*) PR stripping and HF etch and (*f*) stripping of the masking layer.

2.2. Micromachining techniques and process flow

The process started with the RCA cleaning of the glass wafers to free the substrates of organic and inorganic contamination. Selected masking layers (photoresist, Au/Cr, Al, silicon nitride, poly-Si and amorphous silicon) were then deposited onto the glass substrates by using either the PVD physical vapor deposition (PVD) or the chemical vapor deposition (CVD) technique (table 2). For the above non-photoresist masking layers, the standard photolithography technique was used to transfer the pattern onto the additional photoresist layer on the top of the masking layer. This process included spin-coating, soft bake, UV contact exposure, immersion developing and hard bake. Depending on the type of the masking layer, wet chemical etch or RIE was used to transfer the pattern to the masking layer. The wafers were then cut into small pieces for the subsequent glass etch. The HF-based wet etchant including concentrated 49 wt% HF and diluted HF was then used to etch the micro-well into different etch depths at room temperature. At last, the masking layer was removed by either the wet chemical etch or the RIE dry etch to finish the sample preparation (figure 2).

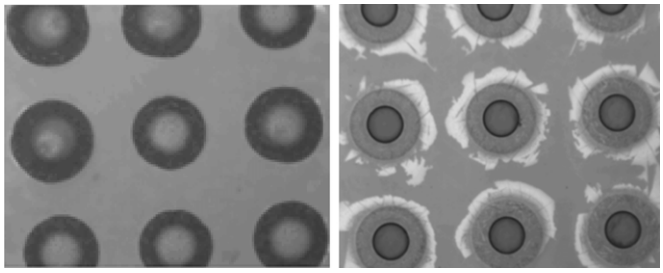

Figure 3. Optical images of a 3 × 3 micro-well array etched in a fused silica substrate by using 8 μm AZP4620 as the etch mask. The left figure shows the result after 50 s etch and the right figure shows the result after 66 s etch. All etches were performed in concentrated 49 wt% HF at room temperature. All micro-wells shown in this figure are 100 μm in diameter.

2.3. Structure profile characterization

The finished samples were examined using both optical microscope and contact stylus profiler. The optical microscope was used to visualize the sample surface and pre-determine whether the etch mask failed after the glass etch. The contact stylus profiler (Dektak 150, Veeco, Tucson, AZ) was used for etch depth measurement and 3D mapping of the well structure. The post-data processing software (VISION from VEECO, Tucson, AZ) was used to perform 3D interactive plot and surface roughness analysis.

3. Results and discussion

3.1. Single masking layer characterization

3.1.1. Photoresist. The PR is well known as the most commonly used masking material in wet chemical etching. However, the interface of the glass photoresist is easy to get penetrated by hydrofluoric acid especially when the concentration of HF increases or deeper etch is performed. Three single-coated photoresists (AZ3312, AZP4620 and AZ5214) with different thicknesses and polarity were selected for this study, and the maximum etching time in a 49 wt% HF etchant which was acquired from 8 μm thick AZ P4620 was estimated to be 1 min. Maximally 1 μm deep etch in a fused silica substrate was acquired from the HF etch without noticeable defects. Any etch beyond this etch depth caused the PR film to start cracking or peel off the substrate (figure 3). This result suggests that alternative masking material needs to be explored to extend the masking layer survival time for deeper etch.

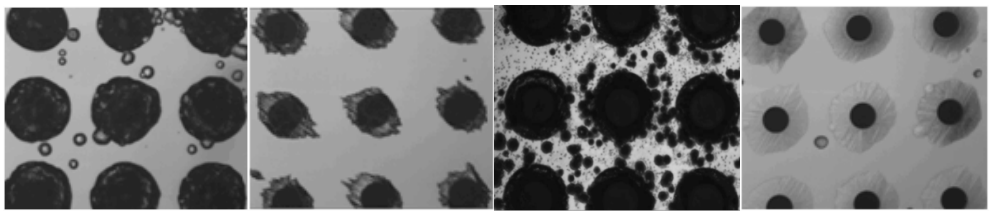

(*a*) (*b*) (*c*) (*d*)

Figure 4. Optical images of micro-wells etched in a fused silica substrate using a metal mask in concentrated HF at room temperature. (*a*) 0.3 μm Au/Cr mask after 3 min etch, (*b*) 0.5 μm Au/Cr after 10 min etch, (*c*) 0.6 μm Al after 1 min etch and (*d*) 1.2 μm Al after 3 min etch. All micro-wells are 100 μm in diameter.

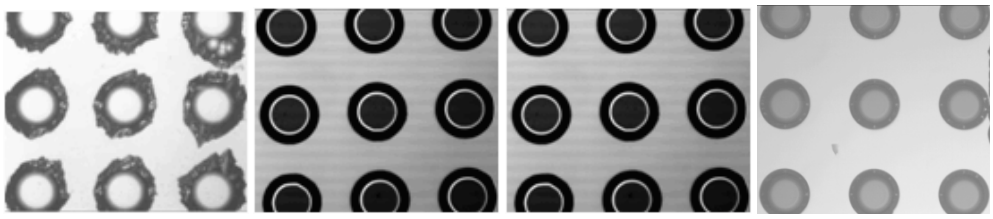

(*a*) (*b*) (*c*) (*d*)

Figure 5. Optical images of micro-wells etched in fused silica masked with silicon-based material after 40 min concentrated HF etch at room temperature. (*a*) 0.5 μm LPCVD poly-Si, (*b*) 0.7 μm LPCVD poly-Si, (*c*) 0.5 μm LPCVD amorphous silicon and (*d*) 0.2 μm LPCVD silicon nitride; all micro-wells are 100 μm in diameter.

3.1.2. Metal. Metal is also widely used in the glass microfabrication process to serve as either the electrical conduction layer or the masking layer. Among various metal layers, Au/Cr has been used as the common masking material for borosilicate glass wet etch since Au is inert in the HF solution. Compared to a photoresist, the glass–Cr interface adhesion appeared stronger which leaded to longer delaminating time, but the pin-hole density was relatively higher for a single-coated Au/Cr layer. Since the Au/Cr thin film is hydrophilic, the HF molecules get absorbed inside the inherent pin holes and cause the enhanced defects on the glass surface (figure 4(*a*)). This issue can be improved to some extent by increasing the gold film thickness (figure 4(*b*)), but the maximum etch time was still very limited. For example, an E-beam evaporated 5000 Å thick Au/Cr thin layer can remain defect free in a concentrated HF solution only for less than 20 min. Though it was reported that the etch time can be increased by annealing the Au/Cr film at 250 °C [13], the resulting Cr–glass adhesion became poor because Au got diffused into the Cr layer which leaded to quick peeling of the masking layer. An alternative method is to keep increasing the Au thickness or form multiple Cr/Au layers [14], but the process will get relatively complicated and expensive. The maximum etch depth acquired by using the single-coated Au/Cr mask was 10 μm for fused silica substrates with relatively lower yield and repeatability.

For comparison, the use of Al as the masking material was also studied since Al is much cheaper than Au and is CMOS process compatible. Figure 4(*c*) shows the etched micro-well with a 0.6 μm Al etch mask after 66 s concentrated HF etch at room temperature. The Al film showed many more pin-hole defects on the surface and edge compared to Au/Cr. Similar to Au/Cr, this issue can be improved by increasing the Al film thickness (figure 4(*d*)), but the Al–glass adhesion was still too weak to prevent the lateral HF penetration for long-time etch. The maximum etch depth acquired by using a single Al masking layer was 3 μm for fused silica substrates.

3.1.3. Silicon-based masking material. Silicon-based thin film is another well-known inert material to HF. Compared to other masking materials, it shows excellent adhesion with the glass substrate, and more importantly, the surface of silicon-based material is hydrophobic [14] which highly prevents the formation of surface pin holes and notching effect during the HF etch. This property implies that this masking material could be a good candidate for deep fused silica etch.

Figure 5 shows a fused silica substrate after 40 min HF etch by masking it with three different silicon-based materials including poly-silicon, amorphous silicon and silicon nitride. Compared to metal and PR, the previously observed pin holes were highly reduced. However, the thickness of the masking layer is critical to reduce the notching effect. For example, 0.5 μm poly-silicon showed clear notching defects (figure 5(*a*)) and these defects were eliminated by increasing the thickness to 0.7 μm (figure 5(*b*)). This can be explained by the residual film stress from the LPCVD process which is directly related to the film thickness. Since the LPCVD process was performed in a high temperature (500–600 °C) furnace, the resulting film stress can be up to 2000 MPa which caused the formation of the notching defects around the etch edge due to the breakage of a highly stressed masking layer during the HF etch. While additional annealing can help to reduce the stress level, selecting the appropriate thickness for different masking layers can also eliminate the notching defects. By selecting 0.2 μm LPCVD silicon nitride or 0.5 μm LPCVD amorphous silicon as the masking material, over 60 μm deep etching was acquired in a fused silica

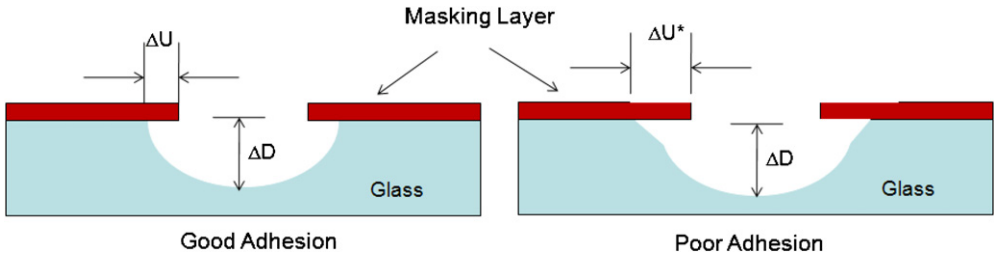

Figure 6. Illustration of the undercut during the HF wet etching. The masking layer with poor adhesion to the glass substrate leads to much increased undercut and tapered side wall.

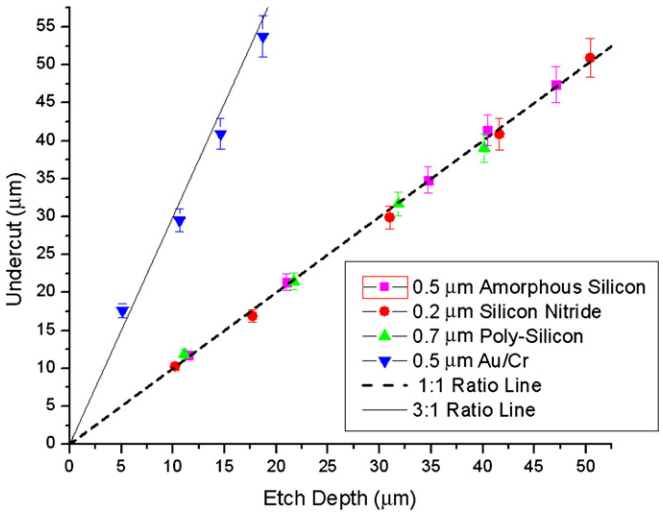

Figure 7. Undercut characterization on a fused silica substrate masked with various materials. All etching are performed in non-diluted HF (49 wt%) at room temperature without agitation.

substrate without any observable pin holes and notching defects.

3.2. Undercut characterization

Due to the isotropic nature of the wet etch, the etched structure always shows a semi-circular wall and the undercut is defined to be the geometry difference between the designed etching window and final opening. In an ideal case, the quantity of the undercut is equal to the etch depth, or the isotropy ratio ($\Delta U/\Delta D$) is 1. However, this ratio depends on the quality of the masking material in term of the interface adhesion. Masking layer with poor adhesion to the glass substrate will lead to a tapered side wall and much increased undercut due to the delaminating of the masking material around the window edge (figure 6).

For shallow etch, this effect is not critical and the final structure geometry is still within the acceptable range. However, as the etch depth goes deeper and deeper, geometry compensation during the structure design has to be made to acquire desired pattern transfer to the glass substrate. Figure 7 shows the amounts of the undercut in the concentrated HF etch by using four different masking materials on a fused silica substrate. For silicon-based material, the isotropy ratio was close to 1 which implied that these materials have excellent adhesion to the glass substrates during the HF etch. For the Au/Cr layer, this ratio increased to 3 which implied that the film delaminated during the HF etch and a tapered wall was formed at the edge of the etching window. For a PR, this ratio has been observed to be up to 10 which implied that the glass–PR adhesion was much weaker compared to other masking materials.

3.3. Etch rate

The etch rate is the most important parameter in the wet-etch technique since it directly determines the time required to get the desired etch depth. In general, the glass etch rate is mainly determined by the glass composition, etchant composition and etching temperature. Since the HF etch at elevated temperature will generate aggressive HF vapor, a related study was not performed due to the safety reason. The results from the study of the other two factors are presented in this paper.

Figure 8(*a*) shows the result of 49 wt% HF etching for three selected glass substrates. As the SiO_2 content inside the glass decreased from 100% (fused silica) to 64% (D-263), a less and less silicate network structure had to be broken by the HF reaction ($SiO_2 + 4HF \rightarrow SiF_4 + 2H_2O$). Therefore, the etch rate dramatically decreased from 36 μm min^{-1} for D-263 to 1 μm min^{-1} for fused silica. The observed etch rate kept was constant for various etch windows (20–250 μm diameter circles) and etch depths (1–60 μm) when using a fresh and stabilized etchant. Figure 8(*b*) shows the effect of adding acids into the etchant on the average etch rate. When acids such as hydrochloric acid and phosphoric acid were added into the HF etchant, the concentration of reactive HF_2^- got reduced which led to the decrease of the etch rate. However, adding acids also increased the H^+ concentration inside the etchant solution which increased the etch rate. These two reactions competed each other during the HF etch which made the overall etching very complicated. For the same acid concentration, the etch rate was determined by the concentration of H^+. Strong acid such as hydrochloric acid introduces more H^+ into the etchant, so the etch rate was higher compared to that of weak acid (H_3PO_4) and non-acidic solution (water). This effect was not obvious on fused silica, but showed a big difference on the D-263 substrate which has a high impurity content because the impurity-oxygen bond is relatively easier to be broken by H^+. The above results have direct impacts on the masking layer selection. For example, the PR and metal cannot be used for >10 μm deep HF etch on fused silica, because these masking materials cannot survive in an HF solution for 10 min. But

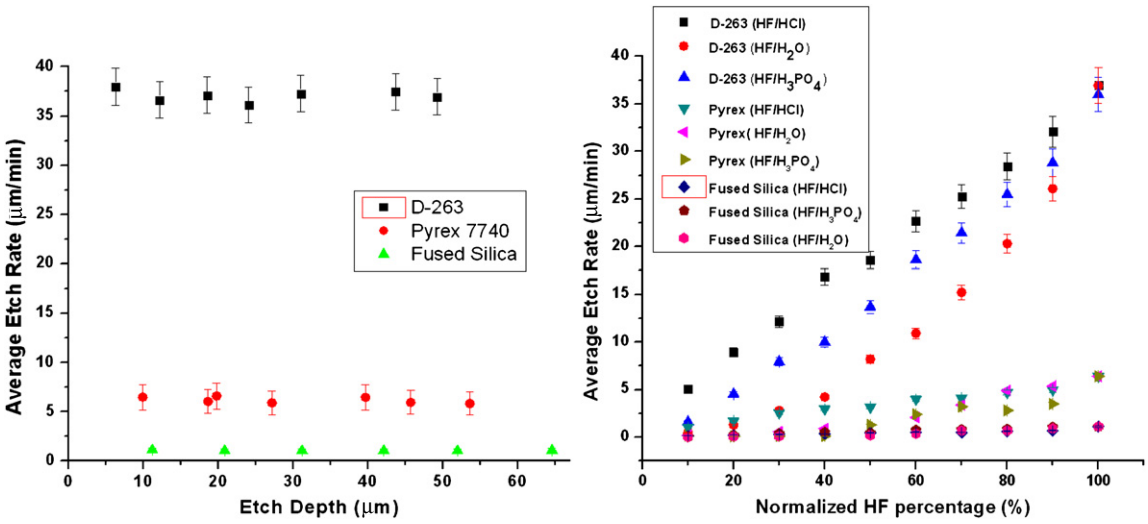

Figure 8. Glass etch rate characterization. (*a*) Average etch rate of three glass substrates in 49 wt% HF and (*b*) average etch rate of three glass substrates in various HF diluting solutions. All etches were performed at room temperature without agitation.

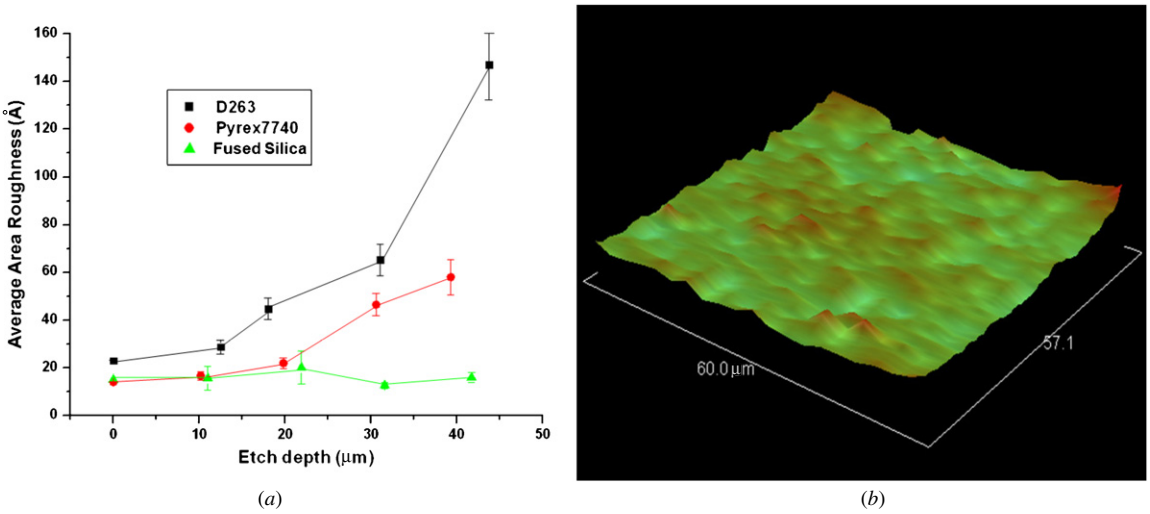

Figure 9. Characterization of the average surface roughness (*Ra*) on (*a*) three substrates at various etch depths and (*b*) fused silica substrate with fixed etch depth (40 μm deep); *Ra* remains constant at 15–20 Å.

they are strong enough to be used for D-263 for deep etch up to 300 μm.

3.4. Surface roughness

The resulting glass surface roughness from the HF wet etch is also very important for precise control of the micro-well volume and reduction of the potential signal 'cross-talking' during the optical sensing experiment. Depending on the impurity concentration inside the glass substrate, the resulting surface roughness can be very different. In general, the insoluble reaction product from the HF etch reaction will form a local etch mask which prevent HF penetration inside the etch area and raise the surface roughness. This can be easily seen from figure 9(*a*). The D-263 substrate which contains over 35% of impurity showed the roughest surface compared to other purer glass substrates at the same etch depth. As the etch depth got deeper and deeper, the roughness increased as well while fused silica showed relative constant roughness since it has near-zero impurity. Figure 9(*b*) shows the average surface roughness (*Ra*) for fused silica after 40 min concentrated HF etch. The measured *Ra* was 15.9 Å for a scan area of 60 μm $\times$ 57 μm. This value was about ten times smaller than that acquired from the D-263 substrate at the same etch depth which implies the advantage of using a fused silica substrate for roughness reduction.

3.5. Fabrication of micro-well array chips and cell/sensor deposition

The acquired results and techniques were successfully applied during the micro-well array fabrication. Figure 10 shows the images of fabricated 3 $\times$ 3 micro-well arrays on a fused silica substrate using 2000 Å LPCVD silicon nitride

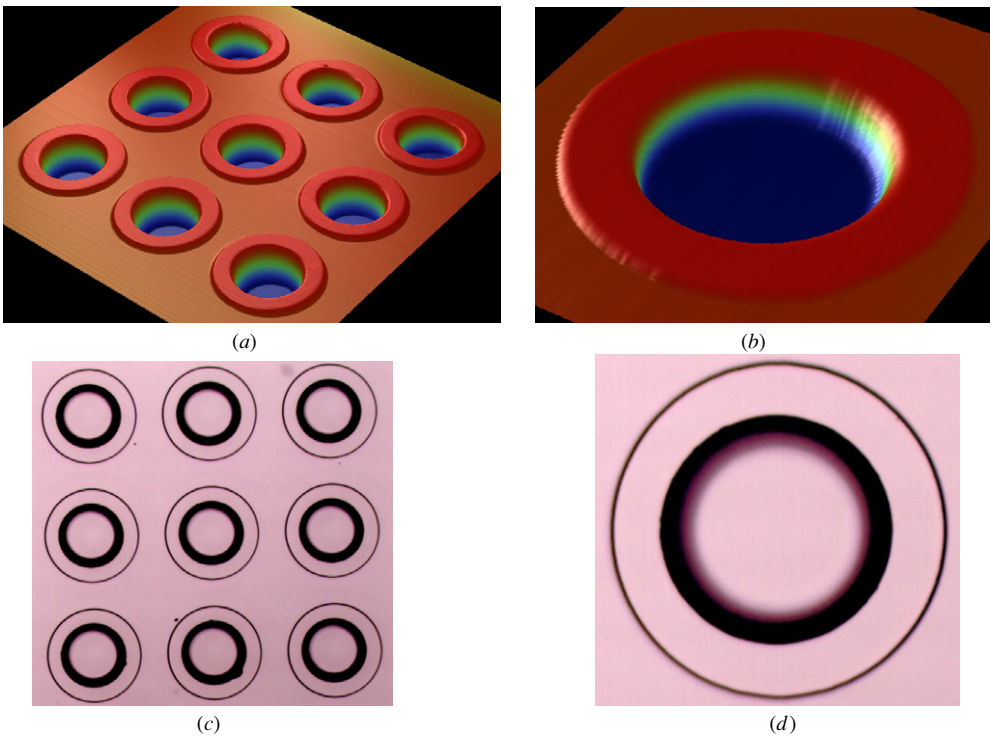

Figure 10. Fabricated micro-well structures on a fused silica substrate. (*a*) 3D contact profile of the 3 × 3 array, (*b*) 3D profile of a single micro-well, (*c*) optical image of a 3 × 3 micro-well array and (*d*) optical image of a single micro-well. All micro-wells are 200 μm in diameter and 40 μm deep.

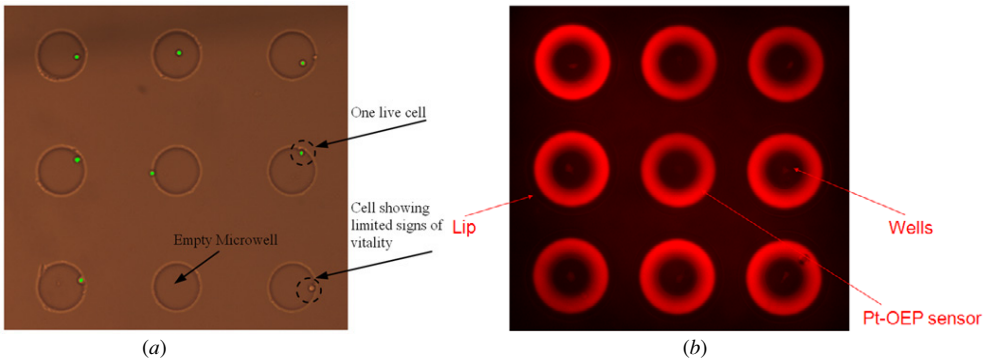

Figure 11. Results from cell trapping and sensor deposition into the fabricated micro-wells. (*a*) A 3 × 3 micro-well array loaded with 8 BE cells and (*b*) a 3 × 3 micro-well array deposited with platinum–porphyrin oxygen sensors.

as the masking layer. Each micro-well is 40 μm deep with 3 μm tall surrounding lips by adding additional lithography and wet-etch process steps into the process flow shown in figure 2. Barrett's esophagus (BE) cells were first stained with Calcein acetoxymethyl (AM) cell-permanent dye that is used to determine cell viability, and were then aspirated and dispensed into each micro-well. Figure 11(*a*) presents a green fluorescent image superimposed on a bright field image, where live cells appear to glow in green. The oxygen sensor (Si/Pt–porphyrin) was dispensed into the micro-wells using the pico injector, and the fluorescence image (figure 11(*b*)) shows that the sensors surround the well edge and form separate O-ring patterns on each micro-well. After cell loading and sensor deposition into the micro-well, the chip was brought to contact with another blank glass chip by applying a constant force of about 18 lbs to completely seal the micro-well; the oxygen inside the micro-well was set to fixed concentration.

The fluorescence was excited at 396 nm using a LED as the light source and detected using a band pass BP650/50 emission filter (Chroma Technology Corp.). The seal quality was tested (indirectly) by observing interference patterns resulting from the deformation caused by the pressure and/or (directly) by monitoring the decrease in oxygen concentration due to oxygen conversion to singlet oxygen by the sensor. In the latter case, an increase in the sensor emission intensity is observed with time if a proper seal is produced. The absolute oxygen concentration can be determined by measuring the intensity ratio between the Pt–porphyrin and Si–porphyrin emission intensities. Because Si–porphyrin does not change its intensity

as the oxygen concentration changes, it is used as a reference for ratiometric oxygen measurements.

4. Conclusion

As conclusion, the deep wet-etching process on a fused silica substrate has been developed and characterized in detail. The pin hole and notching defects of various single-coated masking layers during the concentrated HF etch were characterized, and the most suitable masking material was identified for different etch depths. Single-coated silicon-based thin film with suitable thickness was demonstrated to be the best masking material for deep fused silica etch (>30 μm). To acquire precise pattern transfer to the glass substrate, good adhesion between glass and masking material is desired. The characterization result showed no film delaminating for silicon-based thin film after up to 60 min concentrated HF etch, and the isotropy ratio was close to 1. The average etch rate of fused silica acquired from concentrated 49 wt% HF at room temperature was over 1 μm min^{-1} which is the highest wet-etch rate to our knowledge. Up to 60 μm deep micro-wells have been etched in a fused silica substrate with over 90% process yield and high repeatability. The dependence of the average etch rate on the glass impurity concentration and HF composition were also examined. The etch rate increased with the impurity concentration since a less silicate network needs to be broken by the etchant. The diluting of HF reduced the etch rate dramatically due to the decrease of HF_2^+. The acidity of different acids also impacted the etch rate. Stronger acid introduced more H^+ into the etchant and increased the etch rate compared to weaker acid diluting. The roughness study showed that the average surface roughness was highly depended on the purity of the glass, and the fused silica had constant and the lowest average area roughness (*Ra*) in the range of 15–20 Å compared to other impure substrates. The developed and characterized techniques for deep wet etching of fused silica were successfully implemented in the fabrication of a micro-well array for single cell trapping and sensor deposition and can be easily applied in any other glass-based chip micro-fabrication.

Acknowledgments

The authors would like to thank the CSSER (Center for Solid State Electronic Research) staffs for all their technical help, and Dr Yasser Anis and Dr Laimonas Kelbauskas for the help on the cell/sensor deposition and imaging. This work was supported by a grant from the NIH National Human Genome Research Institute, Centers of Excellence in Genomic Science, Grant Number 5 P50 HG002360, D Meldrum (PI).

References

[1] Lidstrom M E and Meldrum D R 2003 Life-on-a-chip *Nature Rev. Microbiol.* **1** 158–64
[2] Amao Y, Asai K and Okura I 2000 Oxygen sensing based on lifetime of photoexcited triplet state of platinum porphyrin-polystyrene film using time-resolved spectroscopy *J. Porphyrins Phthalocyanines* **4** 292–9
[3] Shonat R D and Kight A C 2003 Oxygen tension imaging in the mouse retina *Ann. Biomed. Eng.* **31** 1084–96
[4] Trettnak W, Kolle C, Reininger F, Dolezal C and O'Leary P 1996 Miniaturized luminescence lifetime-based oxygen sensor instrumentation utilizing a phase modulation technique *Sensors Actuators* B **36** 506–12
[5] Valledor M, Campo J C, Sanchez-Barragan I, Costa-Fernandez J M, Alvarez J C and Sanz-Medel A 2006 Determination of phosphorescence lifetimes in the presence of high background signals using phase-shift measurements *Sensors Actuators* B **113** 249–58
[6] Wilson D F, Grosul P, Rozhkov V, Dugan B W, Reitveld I and Vinogradov S A 2002 Oxygen distributions within tissue by phosphorescence quenching *Proc. SPIE* **4626** 184–92
[7] Molter T W, Holl M R, Dragavon J M, McQuaide S C, Anderson J B, Young A C, Burgess L W, Lidstrom M E and Meldrum D R 2008 A new approach for measuring single-cell oxygen consumption rates *IEEE Trans. Autom. Sci. Eng.* **5** 32–42
[8] Ceriotti L, Weible K, De Rooij N F and Verpoorte E 2003 Rectangular channels for lab-on-a-chip applications *Microelectron. Eng.* **67–68** 865–71
[9] Koutny L B, Schmalzing D, Taylor T A and Fuchs M 1996 Microchip electrophoretic immunoassay for serum *Anal. Chem.* **68** 18–22
[10] Stjernstrom M and Roeraade J 1998 Method for fabrication of microfluidic systems in glass *J. Micromech. Microeng.* **8** 33–8
[11] Grosse A, Grewe M and Fouckhardt H 2001 Deep wet-etching of fused silica glass for hollow capillary optical leaky waveguides in microfluidic devices *J. Micromech. Microeng.* **11** 257–62
[12] Steingoetter I and Fouckhardt H 2005 Deep fused silica wet etching using an Au-free and stress-reduced sputter-deposited Cr hard mask *J. Micromech. Microeng.* **15** 2130–5
[13] Tay F, Iliescu C, Jing J and Miao J 2006 Defect free wet etching through pyrex glass using Cr/Au mask *Microsyst. Technol.* **12** 935–9
[14] Iliescu C, Tay F and Miao J 2007 Strategies in deep wet-etching of pyrex glass *Sensors Actuators* A **133** 395–400